



WP4 D4.2 D10

In situ datasets that couple tracer experiments and geophysical monitoring available

December 2020- Scientific deliverable
Enigma ITN

WP4 – Create new methods for tracking the transport and reactivity of chemical species in subsurface

D4.2/ D10: Public Report: In situ datasets that couple tracer experiments and geophysical monitoring available

Estimated delivery date: 31/12/2020 - Delivery date: 15/01/2021

Lead Beneficiary:

JUELICH: Sander Huisman

UPCH: Majken Looms Zibar

Contributors for this report:

JUELICH: Peleg Haruzi

ULG: Richard Hoffmann

CNRS: Lara Blazevic

Tübingen: Veronika Riekh/Carsten Leven

Objectives of this work package

The objective of work package 4 is to expand our capability to monitor transport and reaction processes in the natural subsurface. This will provide in-situ datasets of particular importance since our conceptual models rely essentially on lab experiments and borehole measurements of chemical species concentrations. The main challenge is to obtain truly quantitative probabilistic estimates of concentration and reaction rate distribution, while coping with the limited spatial resolutions of imaging techniques and the multiple sources of signals associated with transport and reaction processes.

Description of work

The tasks are

- (i) Enhance resolution of time lapse geophysical imaging of transport with new experimental and inversion strategies
- (ii) Develop quantitative inversion of SIP signals induced by biochemical processes
- (iii) Develop an upscaling framework for quantifying the impact of spreading and mixing on geophysical signals

Introduction

In hydrogeology, a tracer is defined as a species (or substance) that can be introduced into a system so that its temporal and spatial distribution or reaction in the subsurface can be monitored. Tracer experiments allow to estimate the groundwater transfer times and parameters that define the aquifer system under consideration (e.g. Ptak et al., 2004; Maliva, 2016). The most widely used tracers are chemical substances. In this case, it is important to select a tracer that is characterized by low natural concentrations in groundwater and a high solubility. Ideally, the tracer also is inert and does not show a density effect. While the first two features are fundamentally, the importance of the latter two features depends on the research purpose. For example, dye tracers typically fulfill all four features, so that these are the favored choice to characterize the advection velocity (or transport velocity in groundwater systems). In contrast, salt tracers can be used to study directly the dynamic change of groundwater levels due to changes of density on groundwater flow or its sensitivity to another imaging technique is used. A reactive tracer allows the observation of chemical reactions in the subsurface. An important condition for a successful tracer experiment is the use of a good analytical instrument with low detection limits, high saturation threshold, high precision, high frequency measurements and the possibility of multiple tracer measurements.

Tracer experiments are an active field of development and new methods are still being proposed and tested, such as tracer experiments with dissolved gases (Brennwald et al., 2016; Chatton et al., 2017; Hoffmann et al., 2020) or heat (i.e. hot water, Read et al., 2013; Wagner et al., 2014; Wildemeersch et al., 2014; Klepikova et al., 2016; De La Bernardie et al., 2018; Sarris et al., 2018). Both are innovative tracers that are characterized by higher diffusion coefficients compared to conventional dye tracers

(Anderson, 2005; Domenico & Schwartz, 1998; Skagius & Neretnieks, 1986). These more diffusive tracers have a complementary nature to conservative tracers and show much higher sensitivity to diffusive processes (i.e. conduction) than to advective dispersion (Irvine et al., 2015; Kurylyk & Irvine, 2019; Hoffmann et al., 2020). In particular, heat as tracer changes dynamically the viscosity and the density of the fluid (Ma & Zheng, 2018; Dassargues 2018). Heat can be transported through the solid matrix and the pores, which allows to investigate zones of low hydraulic conductivity and the immobile water domain compared to a solute tracer that can be transported only through pores and fissures (Irvine et al., 2015; Dassargues 2018).

Tracers can be passively observed or actively injected in the saturated and unsaturated zone. When a tracer test is performed under saturated conditions then it should be preferably be performed under the natural gradient of the aquifer system under consideration. Such tracer tests would provide information about the direction and the different tracer transfer times in the subsurface under the natural hydrological flow regime (Ptak et al., 2004; Maliva, 2016). The estimated or observed transfer times must always interpreted with regard to the used tracer species as well as the porous medium under investigation (Dassargues 2018). For measuring the evolution of concentration or temperature as a function of time, the required instruments are typically installed in the available boreholes of the test site, where a tracer arrival is expected. While a wide range of conventional and reactive tracer tests have been reported, it was noticed that only one heat tracer experiment was performed using a natural gradient so far (Wagner et al., 2014). Other tests were typically performed with active pumping (i.e. under a forced gradient) due to the high dilution of temperature and the fact that the temperature signal may be difficult to catch (Read et al., 2013; Wildemeersch et al., 2014; Klepikova et al., 2016; Sarris et al., 2018; De La Bernardie et al., 2018, 2019; De Schepper et al., 2019; Hermans et al., 2019). This emphasizes the need for heat tracer experiments performed under a natural gradient.

Tracer test are often monitored using a limited number of measurements made at selected locations (e.g. boreholes). Geophysical imaging methods allow to monitor the spatial distribution of a tracer over time with high resolution in terms of concentration and temperature and can more realistically account for spatial heterogeneity. Electrical resistivity tomography (ERT) has been tested for such purposes and in particular for salt (e.g. Kemna et al., 2002) and heat tracing (e.g. Hermans et al., 2015). Ground penetrating radar (GPR) has also been used to image a salt tracer (e.g. Shakas et al., 2016), but has not yet been tested for imaging heat tracer experiments. The infiltration of salt causes an increase in electrical conductivity which results in a decreased GPR signal amplitude, but a change in permittivity is not expected (Sreenivas & Venkatarantan, 1995). The infiltration of a heat tracer causes a decrease in permittivity and an increase in electrical conductivity, which results in a change in both phase and amplitude (Seyfried and Grant, 2007). Compared to ERT, the depth of investigation of GPR is lower, but the resolution is expected to be higher. When GPR data are acquired between two observation wells (crosshole GPR), the resolution of GPR further improves due to a good subsurface illumination with dense ray-coverage. Crosshole GPR has been used to monitor flow and transport in aquifers (Day-Lewis et al., 2003; Looms et al., 2008). This type of GPR set-up has already been used to monitor unsaturated flow and transport (e.g. Looms et al., 2008). Tracers can also be beneficial to identify preferential flowpaths, such as fractures in bedrock, with geophysical methods.

In this deliverable D4.2, we report on the collection of data sets that couple conventional and non-conservative tracer information with geophysical imaging techniques. The first two datasets report on two natural gradient tracer experiments in an alluvial sediment aquifer at the Krauthausen test site in

Germany (Vereecken et al., 2000): (1) a salt injection and (2) heat (i.e. hot water) injection. The fate of both tracer plumes were imaged by time-lapse crosshole GPR. This dataset allows to evaluate the complementary nature of salt and heat (i.e. thermal retardation). The second experiment also allowed to test to what extent the GPR technique can image temperature signals. These two tracer test were performed as a collaborative action within the ITN-ENIGMA network, which provided the broad spectrum of expertise required for these joint experiments. The collaboration allowed to combine the expertise of industrial (Aquale) and scientific partners (as well as their ESR's) in the fields of tracer techniques (ULiege and UMons, ESR 11), concentration and temperature monitoring (URennes 1, ESR 6) and geophysical imaging (FZJ, ESR10).

The third dataset reports on a combined fluorescein and salt tracer test monitored with ERT at the Lauswiesen test site.

The fourth dataset is not strictly a tracer test because it is focussed on infiltration of water into the vadose zone. It is nevertheless included in this deliverable for completeness. As in the case of tracer tests, this dataset illustrates the benefits of time-lapse geophysical monitoring for monitoring the water content development with depth and to study the transition between the unsaturated and saturated zone.

Dataset 1

Salt tracer experiment: Time-lapse crosshole GPR and electrical conductivity log measurements

Author | Contact Person: Peleg Haruzi (p.haruzi@fz-juelich.de), Anja Klotzsche (a.klotzsche@fz-juelich.de).

Access to dataset:

GPR dataset –

<https://teodoor.icg.kfa-juelich.de/geonetwork/apps/search/?uuid=77203027-4338-4850-af58-227c63f05dcf>

* Until publication of the data in a paper, this GPR dataset will be available upon request for a password from the contact persons from the Forschungszentrum Jülich (listed above).

Borehole logging dataset –

<https://teodoor.icg.kfa-juelich.de/geonetwork/apps/search/?uuid=d6bb2a18-1339-47ed-b9fd-81df561ca76b>

Description of test site

Crosshole GPR data was collected before and after injection of a salt (experiment 1) and a heat (experiment 2) tracer in the alluvial terrace sediment of the Krauthausen test site. This test site is located in the southern part of the Lower Rhine Embayment in Germany (Figure 1). It is situated approximately 7 km southeast from the Jülich research centre (FZJ). The test site has an extension of 200 × 70 m. In total, 76 observation wells with a diameter of 50 mm were drilled to a depth of about 11 m (Vereecken et al., 2000). The aquifer is limited by flood plain deposits at the top and a clay layer at the bottom. The aquifer consists mainly of gravelly and sandy sediments (Figure 1c). The clay and silt content of the aquifer sediments varies between 0.5 % and 7.5 %, and the mean total porosity is 26 % with a standard deviation of 7 % (Vereecken et al., 2000). The groundwater level at the Krauthausen test site varies through the year from 1-3 m below ground surface. The mean natural hydraulic gradient at the site is 0.002 in NNW direction (Vereecken et al., 2000). The site was investigated in multiple studies using hydrogeological characterization, and transport analysis using soil sampling, geophysical imaging methods, pumping and tracer tests (Döring, 1997, Vereecken et al., 2000, Vanderborght and Vereecken, 2001, Kemna et al., 2002, Englert et al., 2003, Li et al., 2008, Tillman et al., 2008, Müller et al., 2010, Oberröhrmann et al., 2013, Gueting et al., 2015, 2017, 2018, 2020, Kelter et al., 2018).



Figure 1: Krauthausen test site. a) Location of the test site in western Germany (red dot). b) Image collected during GPR crosshole acquisition. c) Generalized cross-section of the investigated aquifer at the Krauthausen test site (modified from Englert, 2003).

Description of the dataset

In the salt tracer test, 4 m³ of water with an electrical conductivity (EC) of about 12 S/m (equals an EC anomaly of around $\Delta EC = 11$ S/m) was injected into the well B29 (Figure 2). The injection flow rate was about 2 m³ h⁻¹ and was determined by a pump meter in order to maintain the desired injection EC constantly. Two borehole EC sensors were used in this experiment that spanned 30 days. One logger was fixed in borehole 34 at 8.5 m depth (breakthrough curve in Figure 3). The second logger was used to obtain EC depth profiles in boreholes 31, 32, 29, 34 (Example for Day 9 in Figure 4).

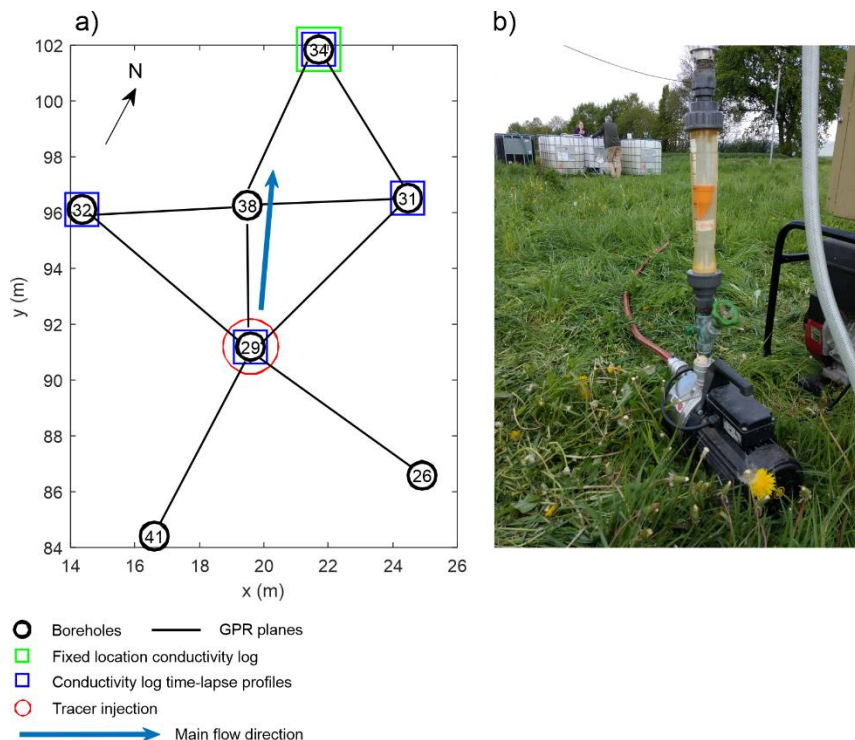


Figure 2: a) Map of the salt tracer test configuration in Krauthausen test site. b) Water pump connected to a flow rate meter for quality control.

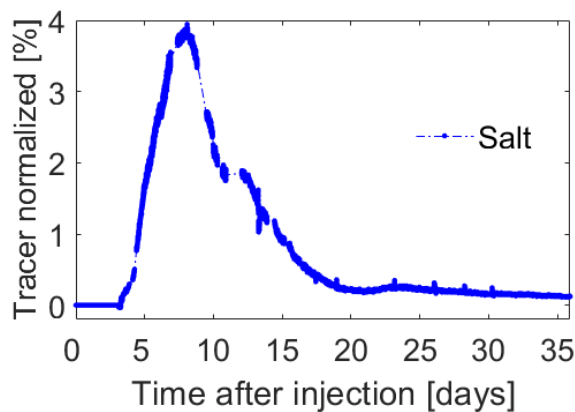


Figure 3: Breakthrough curve from the fixed EC logger in borehole 34 at 8.5 m depth.

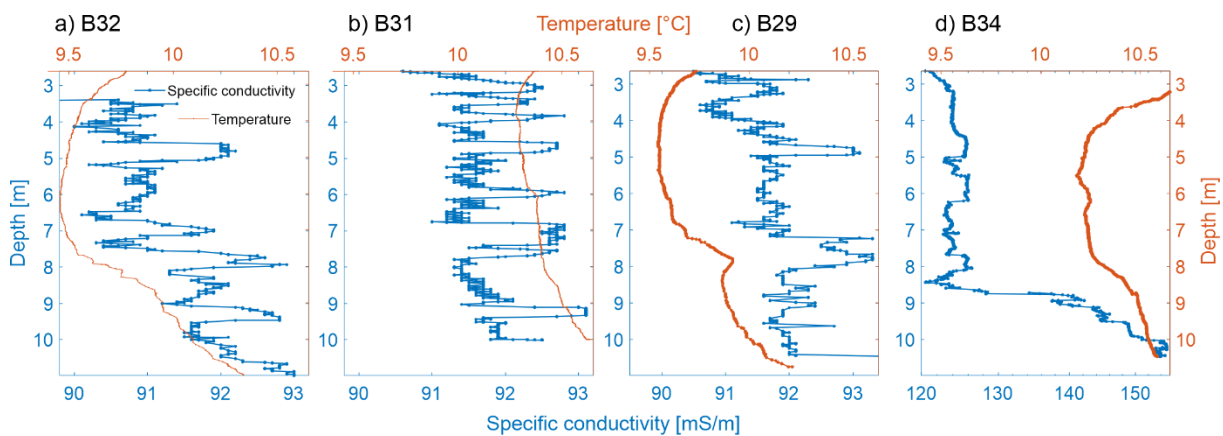


Figure 4: Specific conductivity at 25 °C and temperatures depth profiles for boreholes 32, 31, 29 and 34 at day 9. Background electrical conductivity was about 91 mS/m. Depth was calculated from the logger pressure, the barometric pressure (measured with the sensor above the water level), and the measured water level.

GPR measurements were acquired using a crosshole setup before (background) and after (time-lapse) salt tracer injection. In total, nine crosshole GPR measurement planes were measured (Figure 2a) with 100 (planes 2941, 2926, 2931, 2932) and 200 MHz (planes 2938, 3138, 3832, 3834, 3134) antenna on 42 different times in a time span of 14 days. Each crosshole GPR measurement was acquired in a multi-offset gather (MOG) reciprocal setup using borehole depths between 2.7 and 10.5 m. For the background acquisition, the transmitter spacing was 0.2 m for all measurement planes. For the time-lapse monitoring, the transmitter spacing generally was 0.4 m in order to speed up the data acquisition. A transmitter spacing of 0.2 m was used at locations where we assumed the presence of the salt plume based on the data from the previous day. For both background and time-lapse acquisitions, the receiver spacing was 0.1 m. This results in approximately 40-70 transmitter shot gathers per crosshole measurement. Before and after each MOG, calibration measurements in air were performed. In addition, ZOP (zero-offset profile) of 0.1 m spacing were also used for MOG calibration (Oberröhrmann et al., 2013), and for use in time-lapse ZOP analysis which allowed temporal 1D profiles based on the recorded trace energy.

The effect of the salt tracer on the GPR measurements is illustrated in Figure 5. After 7 days, the GPR signal measured between boreholes B38 and B34 shows lower amplitude due to the high electrical conductivity of the salt. This effect is especially observed below 8 m, where borehole electrical conductivity loggers in B34 measured high electrical conductivity (Figure 4d). On day 11, the GPR signal increased compared to day 7, reflecting a partly recovery of the aquifer from the salt tracer. Permittivity and electrical conductivity models processed by FWI calculated from GPR data before the injection provide dm-scale resolution (Figure 6). Time-lapse GPR data are currently being processed using FWI and will be published as soon as possible.

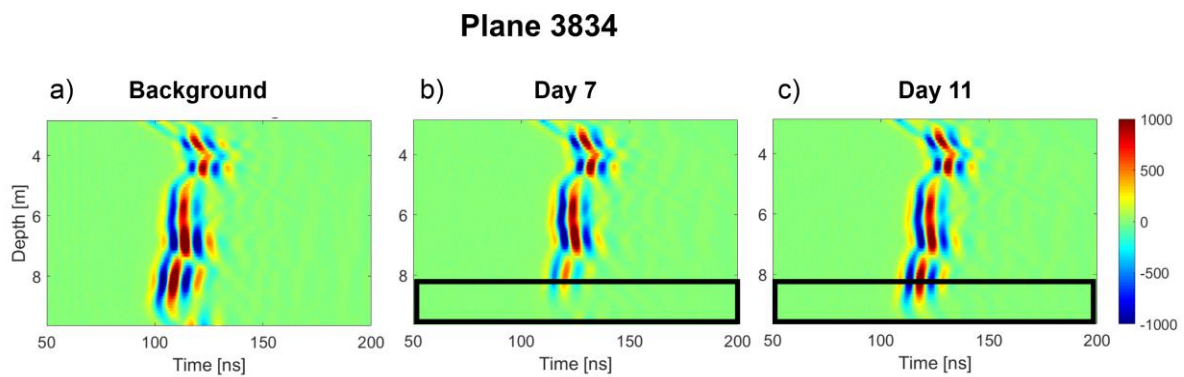


Figure 5: GPR image scan measured between boreholes B38 and B34 in zero-offset profile (ZOP) (a) before the tracer injection, (b) 7 days and (c) 11 days after injection.

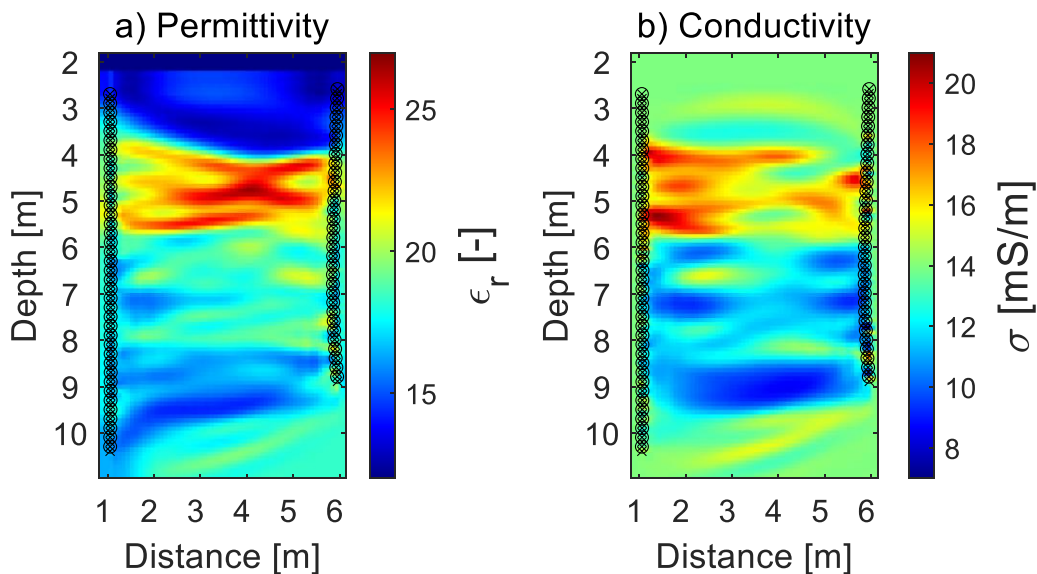


Figure 6: GPR FWI results for GPR datasets acquired before the injection. Transmitter and receiver locations are indicated by 'o' and 'x', respectively.

Description of data files:

- GPR datasets:
 - GPR data of a single dataset is composed of multiples files ("LinesXX.DT1" binary format). Header data is provided ("LinesXX.HD" format).
 - An Excel sheet in each dataset include information on acquisition setup: antenna locations, sampling interval, number of samples.
- Electrical conductivity data from borehole loggers:
 - Data files are stored as time series. More information will be added to the dataset after the complete dataset will be processed.

Each dataset includes README file with more relevant information for processing the data. Contact details of the campaign operators are provided.

Link to field site description:

The following webpage describes the test site and legacy data from the Krauthausen test site.

<https://teodoor.icg.kfa-juelich.de/geonetwork/apps/search/?uuid=ad404c9f-419a-4b14-b6e0-6ee9acd8f80e>

Link to publications: not published yet.

Dataset 2

Hot water tracer experiment: Time-lapse crosshole GPR and temperature measurements.

Author | Contact Person: Peleg Haruzi (p.haruzi@fz-juelich.de), Richard Hoffmann (richard.hoffmann@uliege.be) Behzad Pouladi (behzad.pouladi@gmail.com), Anja Klotzsche (a.klotzsche@fz-juelich.de).

Access to dataset:

GPR dataset –

<https://teodoor.icg.kfa-juelich.de/geonetwork/apps/search/?uuid=01adc209-916b-4ea0-bce7-7ac099d8bde2>

* Until publication of the data in a paper, this GPR dataset will be available upon request for a password from the contact persons from the Forschungszentrum Jülich (listed above).

Borehole logging dataset –

<https://teodoor.icg.kfa-juelich.de/geonetwork/apps/search/?uuid=09a4f00f-d621-4aea-aaeb-efdeea447508>

Description of the dataset:

The Krauthausen test site is described in the context of dataset 1. The wells at this test site consist of PVC pipes, which have a temperature resistance of around 45 °C and are mostly screened over the full aquifer thickness. In this heat tracing experiment, 36 m³ of hot water with a temperature of 44 °C (equals a temperature anomaly of around $\Delta T = 34$ °C) was injected into well B29 (Figure 7, 8). The injection flow rate was 1.8 m³ h⁻¹ and was determined by the portable water heater used in order to maintain the desired constant injection temperature. The evolution of temperature as a function of time (in total 54 days) was monitored with high resolution loggers installed in the wells 29 (Figure 8), 31, 32, 38, 33, 34 and 67 (0.001 °C) (Figure 9, 10). The loggers were installed in different depths in order to monitor the temperature anomalies with depth. This heat tracer experiment was complemented by geophysical imaging using GPR.

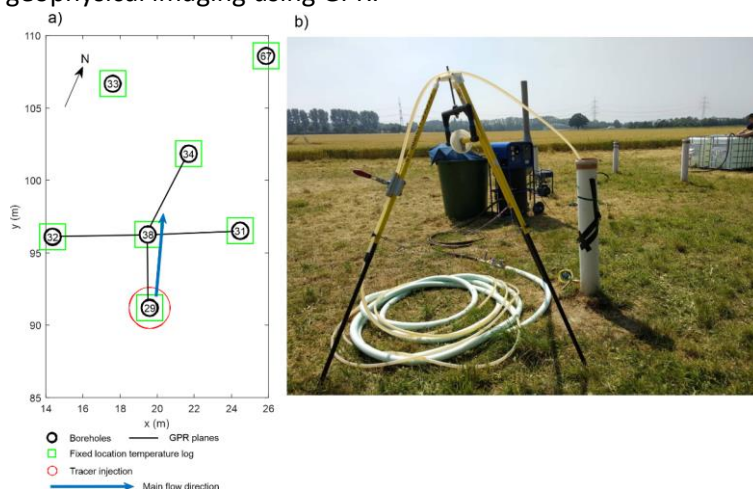


Figure 7: (a) Map of the boreholes used in the heat tracer test at the Krauthausen test site. (b) Field site photo showing the injection system

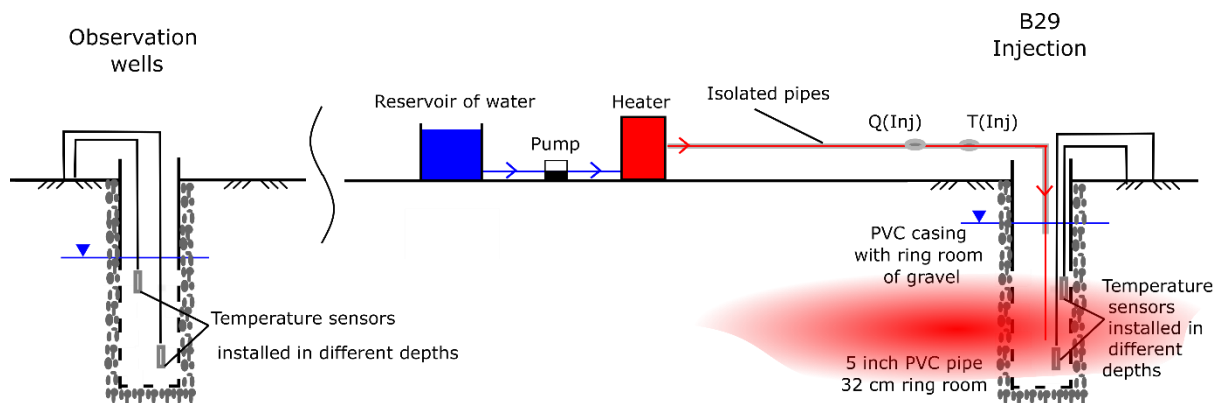


Figure 8: Schematic visualization of the heat tracing experiment conducted under the natural hydraulic gradient of the Krauthausen test site.

GPR measurements were acquired in a crosshole setup before (background) and after (time-lapse) the described hot water tracer injection. In this experiment, four crosshole planes were measured (Figure 7a) with 200 MHz antenna. The dataset includes 39 crosshole measurements acquired in a span of 36 days. Each crosshole measurement was acquired in a multi-offset gather reciprocal setup between depths of 2.7 and 10.5 m. The transmitter spacing was 0.4 m, and the receiver spacing was 0.1 m. This resulted in approximately 40 transmitter shot gathers per crosshole measurement. Before and after each measuring each plane, MOG calibration measurements in air were performed. In addition, ZOP measurements with a 0.1 m spacing were made for MOG calibration (Oberröhrmann et al., 2013), and for use in time-lapse ZOP analysis to obtain 1D profiles based on the recorded trace energy.

Some preliminary interpretations of the raw temperature information show the possible delay of the heat tracer compared to the solute tracer (for borehole 34, Figure 3 and Figure 10d), which is probably related to the effect of thermal retardation. This will be further investigated using the information from the other loggers and from the GPR measurements. The effect of the heat tracer on the GPR parameters in the aquifer is shown in Figure 11. A velocity increase due to the lower permittivity of hot water was apparent until day 9, whereas day 27 shows partially recovery of the aquifer from the heat tracer. This trend is consistent with the temperature breakthrough in B38 (Figure 10c). Background and time-lapse GPR data are being processed using FWI and will be published in a future article.

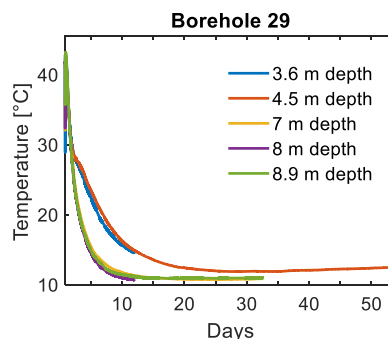


Figure 9: Raw temperature monitored in injection borehole 29 at 5 different depths. Temperatures of injected heat tracer and groundwater were around 44 °C and 10 °C, respectively. Temperature curves are shown starting from the end of the injection.

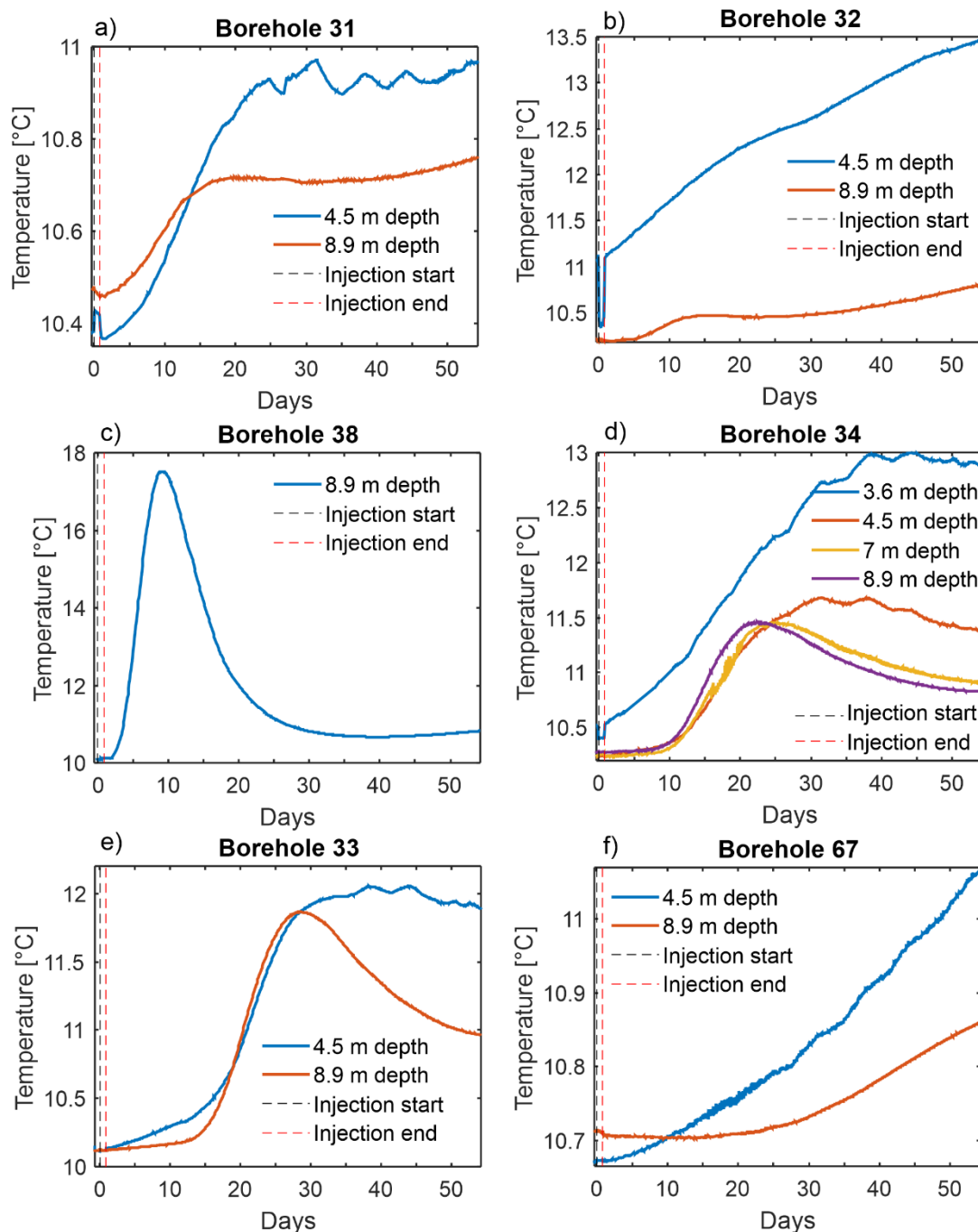


Figure 10: Raw temperature breakthroughs curve in monitoring boreholes. All boreholes are screened except of borehole 38, where the PVC tube is not screened to the aquifer, thus the heat tracer was transported to the tube through the PVC.

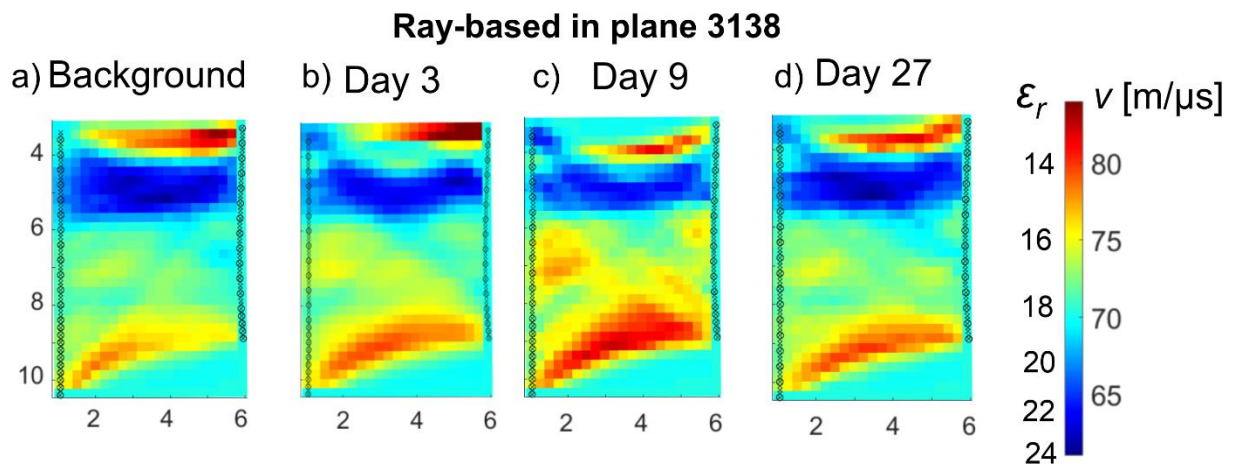


Figure 11: Velocity tomograms measured between boreholes B38 and B31 processed by signal first arrival ray-based inversion. (a) Before injection, and after (b) 3, (c) 9 and (d) 27 days after the beginning of the injection.

Description of data files:

- GPR datasets:
 - GPR data of a single dataset is composed of multiples files ("LinesXX.DT1" binary format). Header data is provided ("LinesXX.HD" format).
 - An excelsheet in each dataset include information on acquisition setup: antenna locations, sampling interval, number of samples.
- Temperature data from borehole loggers:
 - Data files are stored as time series. Three types of loggers were used.

Each dataset includes README file with more relevant information for processing the data. Contact details of the campaign operators are provided.

Link to field site description:

The following webpage describes the test site and legacy data from the Krauthausen test site.

<https://teodoor.icg.kfa-juelich.de/geonetwork/apps/search/?uuid=ad404c9f-419a-4b14-b6e0-6ee9acd8f80e>

Link to publications: not published yet.

Dataset 3

In-situ data sets on 3D-tracer tests with ERT time lapse monitoring on the Lauswiesen test site

Author | Contact Person: Veronika Rieckh (veronika.rieckh@uni-tuebingen.de); Olaf A. Cirpka (olaf.cirpka@uni-tuebingen.de); Carsten Leven (carsten.leven@uni-tuebingen.de)

Access to dataset: The data sets are stored on the CAMPOS data management system and will be made available after publishing the research results on <https://fdat.escience.uni-tuebingen.de/portal/#/start>

Description of the dataset:

A Fluorescein and salt tracer test was monitored with ERT on the Lauswiesen test site. The test set-up consisted of nested, double dipole flow field with an outer injection/extraction well couple (B2-B7) and an inner injection/extraction well couple (B3-B6) (Figure 12-14). A well field with 4 x 4 groundwater wells ("E" wells) was used for tracer and head monitoring. Four out of the 16 wells are multi-level groundwater wells (CMT wells), the remaining wells are fully screened and have a well diameter of 19 mm (3/4"). Along the central line, four fully-screened groundwater well ("K" wells) are installed. Well F0 is used for supplying injection wells. The tracer injection (fluorescein and salt) occurred in the inner injection well, either over the entire water saturated thickness or in an injection interval separated by a double-packer system. The double-packer system was installed in the inner injection well. The packer separated three injection interval: a top, a middle, and a lower interval. Ambient groundwater is always injected in all three intervals, and in the respective tracer interval the tracer is added. The fluorescein and salt tracers were mixed with approx. 4 m³ of water before being injected in the injection interval, while the injection is done using a bypass to not disturb the injection-extraction rates regime, i.e. without changing the total injection rate. Thus, the tracer is injected in a (quasi-)steady state flow field. The transient head data to reach the steady flow field is recorded in several (multi-)level wells. ERT monitoring of the salt tracer breakthrough was recorded using a SYSCAL PRO system with borehole electrodes that were placed in the monitoring wells. Fluorescein monitoring in the observation wells was performed with a 19-channel fluorimeter, and samples were taken regularly and analyzed in the lab for tracer concentration for the calibration of the fluorimeter signals.

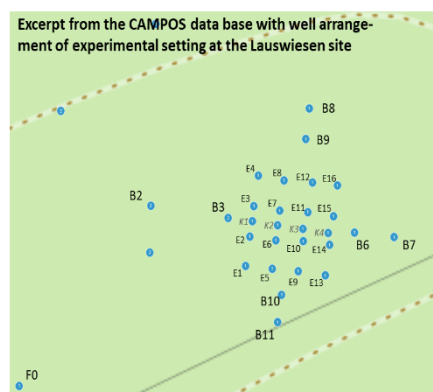


Figure 12. Well arrangement at the Lauswiesen test site.



Figure 13. Impressions from the field site during the tracer test. Four tracer mixing tanks were prepared for tracer injection (green = fluorescein).

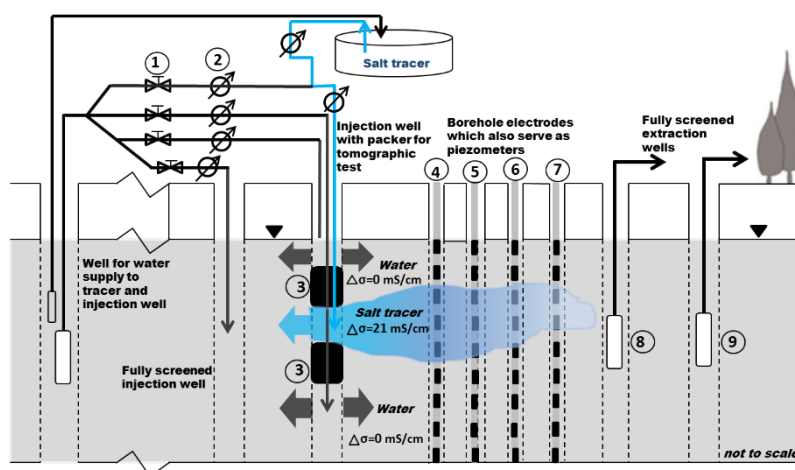


Figure 14. Schematic illustration of the tracer tests at the Lauswiesen test site.

Description of data files:

Five data subsets are available, where each describes one single tracer experiment (=test):

1. Test "FullBorehole_B3-B6"

Tracer injection in B3 over the entire saturated thickness of the aquifer, test parallel and in direction of groundwater flow

File: "Tracer_FullBorehole_B3-B6"

2. Test "FullBorehole_reversed_B6-B3"

Tracer injection in B6 over the entire saturated thickness of the aquifer, test parallel against the direction of groundwater flow

File: "Tracer_FullBorehole_reversed_B6-B3"

3. Test “Tracer InjectionTop B3-B6”

Tracer injection in B3 in the top part of the aquifer, test parallel and in direction of groundwater flow

File: “Tracer_InjectionTop_B3-B6”

4. Test “Tracer InjectionMiddle B3-B6”

Tracer injection in B3 in the middle part of the aquifer, test parallel and in direction of groundwater flow

File: “Tracer_InjectionMiddle_B3-B6”

5. Test “Tracer InjectionBottom B3-B6”

Tracer injection in B3 in the bottom part of the aquifer, test parallel and in direction of groundwater flow

File: “Tracer_InjectionBottom_B3-B6”

The data are stored according to the CAMPOS guidelines on data management. For each experimental data set, a metadata file is available (using the above cited test names) based on the metadata template “SpatialPointData” which is accompanied by a ZIP file containing a text file (TestSetup_***.txt) summarizing all required information on the tracer test itself, and the following folders containing the experimental results (raw and processed data):

- folder “rates” with time series of injection and extraction rates
- folder “headdata” with time series of hydraulic head changes
- folder “tracer” with time series recording by the fluorometer
- folder “samples” with lab measurement data on fluorescein concentrations of samples taken during the test
- folder “ERT” with time-lapse electrical resistivity tomography measurements

The data will be available to the public after they have been published.

Link to publications: not published yet.

Dataset 4

Water infiltration and time-lapse geophysical monitoring of the vadose zone at the Ploemeur Hydrological Observatory (Brittany, France)

Authors | Contact person: Lara A. Blazevic (lara.blazevic@sorbonne-universite.fr), Ludovic Bodet (ludovic.bodet@sorbonne-universite.fr), Sylvain Pasquet (pasquet@ipgp.fr), Niklas Linde (niklas.linde@unil.ch), Damien Jougnot (damien.jougnot@sorbonne-universite.fr), Laurent Longuevergne (laurent.longuevergne@univ-rennes1.fr).

Access to dataset: <http://hplus.ore.fr/en/blazevic-et-al-2020-water-data>

Description of the dataset:

An infiltration of plain water was complemented by time time-lapse geophysical monitoring of the vadose zone at the Ploemeur Hydrological Observatory (Brittany, France). The dataset includes water content data as measured by time domain reflectometry (TDR) probes in the subsurface, raw electrical resistivity and seismic traveltime files, topography files, and electrical resistivity and picked seismic traveltimes files in pygimli format (<https://www.pygimli.org/>) and corresponding inversion results for both geophysical methods. The geophysical acquisition setup consisted of two orthogonal lines crossing at the center of the infiltration area (2.2x2.4m²). For each method, there were 72 sensors (electrodes and geophones) along each line spaced by 20 cm, resulting in 14.2 m-long lines. For the electrical resistivity measurements, we used the Wenner-Schlumberger array type. For the seismic data acquisition, there were 14 shots along each line. Figure 15 shows a schematic of the acquisition setup. The geophysical acquisitions were done after each water infiltration (approximately 400 L per infiltration). In total, there were eleven geophysical acquisitions (for each method) and nine water infiltrations (totaling 3 321 dm³ of infiltrated water). The first acquisition took place before any infiltration (background), the fifth acquisition is the last of day 1, the sixth acquisition is the first of day 2 before infiltrating again, and the eleventh acquisition is the overall last after the last infiltration. Six TDR probes in the subsurface, adjacent to the infiltration area and at different depths, measured the water content continuously and in real-time throughout the experiment. Figure 16 shows the water content evolution as measured by these TDR probes together with a cross-sectional sketch of the TDR probes setup in the subsurface. The analysis of the time-lapse geophysical responses and their implication for the use of seismic methods in near-surface unsaturated contexts are further developed in Blazevic et al. (2020).

Link to field site description: <http://hplus.ore.fr/en/ploemeur/data-ploemeur>

Link to publication: <https://www.mdpi.com/2073-4441/12/5/1230>

References:

Blazevic, L.A.; Bodet, L.; Pasquet, S.; Linde, N.; Jougnot, D.; Longuevergne, L. Time-Lapse Seismic and Electrical Monitoring of the Vadose Zone during a Controlled Infiltration Experiment at the Ploemeur Hydrological Observatory, France. *Water* **2020**, *12*, 1230. doi: <https://doi.org/10.3390/w12051230>

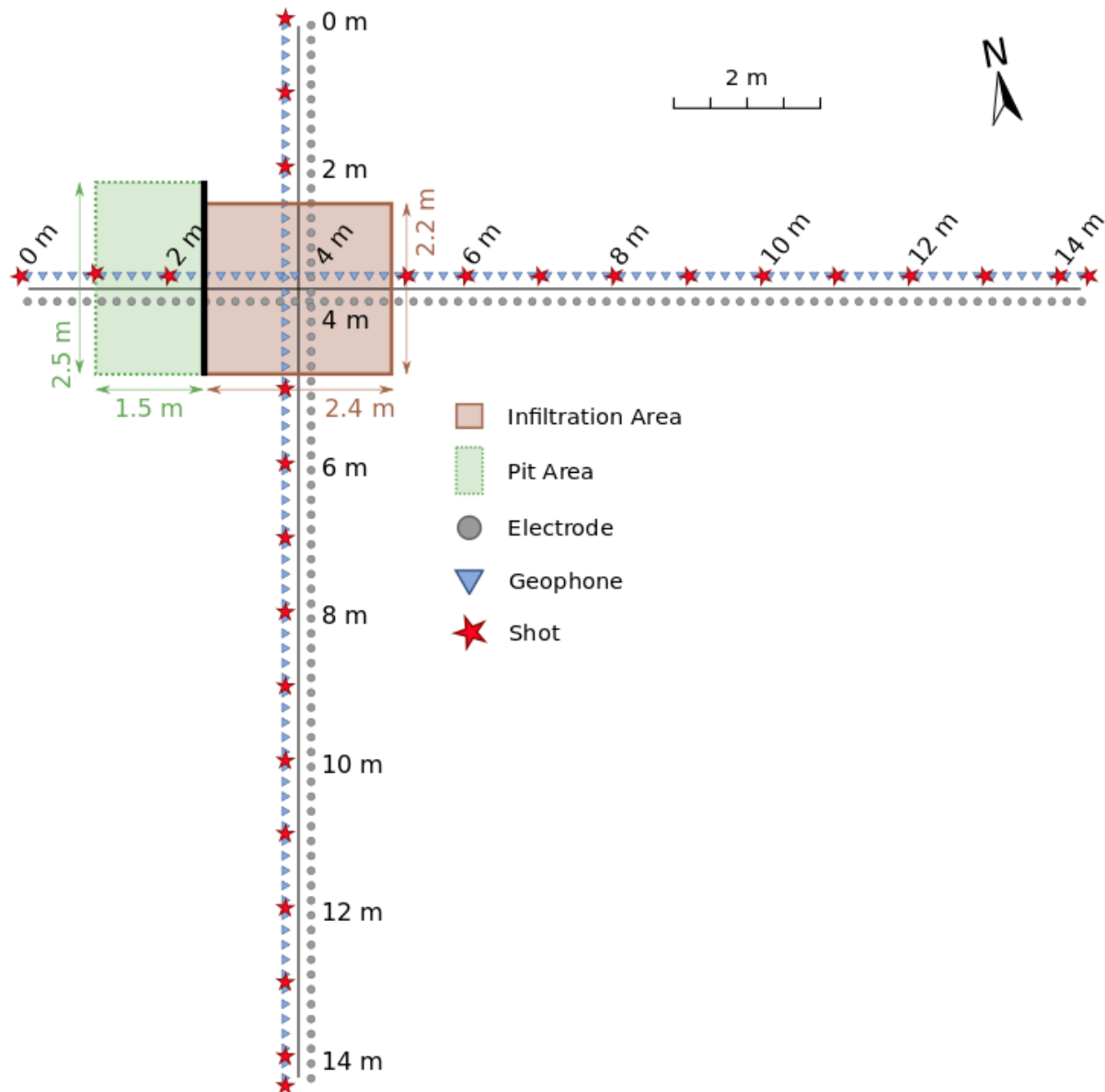


Figure 15. Schematic of acquisition setup. The solid black line along the pit area corresponds to the plane including the buried sensors (see Figure 12(b)). After Blazevic et al. (2020).

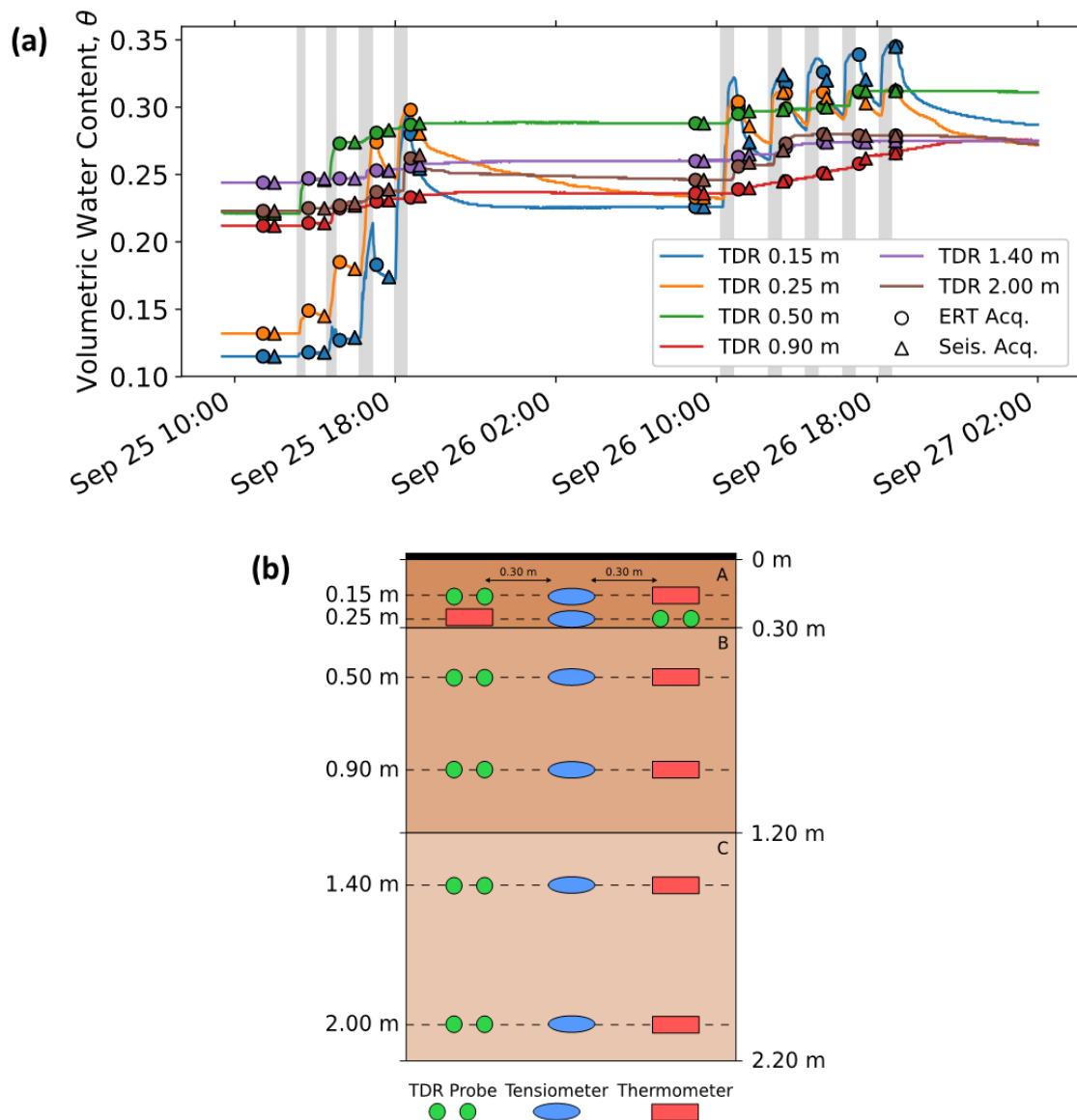


Figure 16. (a) Volumetric water content (θ) throughout the experiment as recorded from the TDR sensors at different depths. Markers indicating starting times of electrical resistivity tomography (ERT) and seismic acquisitions are shown on each curve. Gray shadings correspond to the periods of water infiltration. (b) Cross-section schematic of buried sensors; A, B, and C indicate different soil layers in the subsurface (after Blazevic et al., 2020).

Description of data files:

The ERT, seismic, and water content data are stored in the H+ database (see **Access to dataset**) and can be downloaded after creating a user profile. In this report, we provide a short description of these data files. More detailed descriptions can be found in the H+ database when downloading the data files.

1. ERT files description

Name of raw data files: ERT_NS_step#.bin or ERT_WE_step#.bin

Content of raw data files: xA, xB, xM, xN, Rho, Dev, M, SP, VMN, IAB, Date

Name of localization files: topo_NS.txt, topo_WE.txt

Content of localization files: Topography (x, z) along NS and WE profiles.

Name of inverse data files: ERT_NS_step#.vtk or ERT_WE_step#.vtk

Content of inverse data files: Resistivity (Ohm.m) profiles, Relative change in resistivity with respect to 1st acquisition.

Comments: Files in the *bin* and *Res2dinv* folders are raw (all data points). Files in the *pygimli* folder are without bad data points and with topography for time-lapse inversion using the pygimli library (<https://www.pygimli.org/>). For time-lapse purposes, no bad data points means that if a point was bad for a given acquisition, that point would be deleted from all the acquisitions in that profile (regardless of it being good at other acquisitions). Files in the *Inverted* folder contain the inversion results (both resistivity and relative change profiles) in .vtk format (can be visualized in ParaView <https://www.paraview.org/>).

2. Seismic files description

Name of raw data files: 'Line number (1=NS, 2=WE)' 'Acquisition number' 'Shot number'. E.g.: 1204 = 4th shot, 2nd acquisition, NS line; 21012 = 12th shot, 10th acquisition, WE line.

Content of raw data files: Seismic data (travel times and amplitudes) in seg2 format.

Name of localization files: topo_NS.txt, topo_WE.txt

Content of localization files: Topography (x, z) along NS and WE profiles.

Name of inverse data files: SEISMIC_NS_step#.vtk or SEISMIC_WE_step#.vtk

Content of inverse data files: P-wave velocity (m/s) profiles, Relative change in P-wave velocity with respect to 1st acquisition.

Comments: The two profiles are connected together so each file has 144 traces, for shots along the NS profile read only traces 1-72, for shots along the WE profile read only traces 73-144. Files in the *NS* and *WE* folders are the raw files.

Refracted P-wave first arrival times were picked manually for each shot in each acquisition. Files in the *pygimli* folder contain these picked travel times and topography for time-lapse inversion using the pygimli library (<https://www.pygimli.org/>). Files in the *Inverted* folder contain the inversion results (both P-wave velocity and relative change profiles) in .vtk format (can be visualized in ParaView <https://www.paraview.org/>).

3. Water content file description

A .csv file containing TDR positions in the subsurface (reference elevation and relative depth), date and time, and water content readings throughout the experiment.

REFERENCES

- Anderson, M. P. (2005). Heat as a Ground Water Tracer. *Ground Water*, 43(6), 951–968.
- Brennwald, M. S., Schmidt, M., Oser, J., & Kipfer, R. (2016). A Portable and Autonomous Mass Spectrometric System for On-Site Environmental Gas Analysis. *Environmental Science & Technology*, 50(24), 13455–13463.
- Chatton, E., Labasque, T., de La Bernardie, J., Guihéneuf, N., Bour, O., & Aquilina, L. (2017). Field Continuous Measurement of Dissolved Gases with a CF-MIMS: Applications to the Physics and Biogeochemistry of Groundwater Flow. *Environmental Science & Technology*, 51(2), 846–854.
- Dassargues, A. (2018). *Hydrogeology: Groundwater science and engineering* (1st). Boca Raton: CRC Press.
- Day-Lewis, F. D., Lane Jr, J. W., Harris, J. M., & Gorelick, S. M. (2003). Time-lapse imaging of saline-tracer transport in fractured rock using difference-attenuation radar tomography. *Water Resources Research*, 39(10).
- De La Bernardie, J., Bour, O., Guihéneuf, N., Chatton, E., Longuevergne, L., & Le Borgne, T. (2019). Dipole and Convergent Single-Well Thermal Tracer Tests for Characterizing the Effect of Flow Configuration on Thermal Recovery. *Geosciences*, 9(10), 440.
- De La Bernardie, J., Bour, O., Le Borgne, T., Guihéneuf, N., Chatton, E., Labasque, T., et al. (2018). Thermal Attenuation and Lag Time in Fractured Rock: Theory and Field Measurements From Joint Heat and Solute Tracer Tests. *Water Resources Research*, 54(12), 10053–10075.
- De Schepper, G., Paulus, C., Bolly, P.-Y., Hermans, T., Lesparre, N., & Robert, T. (2019). Assessment of short-term aquifer thermal energy storage for demand-side management perspectives: Experimental and numerical developments. *Applied Energy*, 242, 534–546.
- Domenico, P. A., & Schwartz, F. W. (1998). *Physical and Chemical Hydrogeology, 2nd Edition*. New York: John Wiley & Sons Inc. Retrieved from <http://www.wiley.com/WileyCDA/WileyTitle/productCd-0471597627.html>
- Döring, U. (1997). *Transport of the reactive substances eosin, uranine and lithium in a heterogeneous aquifer*. Doctoral dissertation, Christian-Albrechts Universität, Kiel, Germany.
- Englert, A. (2003). *Measurement, estimation and modelling of groundwater flow velocity at Krauthausen test site*. Doctoral dissertation, RWTH Aachen, Germany.
- Gueting, N., Caers, J., Comunian, A., Vanderborght, J., & Englert, A. (2018). Reconstruction of three-dimensional aquifer heterogeneity from two-dimensional geophysical data. *Mathematical Geosciences*, 50(1), 53–75.
- Gueting, N., Klotzsche, A., van der Kruk, J., Vanderborght, J., Vereecken, H., & Englert, A. (2015). Imaging and characterization of facies heterogeneity in an alluvial aquifer using GPR full-waveform inversion and cone penetration tests. *Journal of Hydrology*, 524, 680–695.
- Gueting, N., Klotzsche, A., van der Kruk, J., Vanderborght, J., Vereecken, H., & Englert, A. (2020). Corrigendum to "Imaging and characterization of facies heterogeneity in an alluvial aquifer using GPR full-waveform inversion and cone penetration tests"[*J. Hydrol.* (2015) 680–695]. *Journal of Hydrology*, 590, 125483.
- Gueting, N., Vienken, T., Klotzsche, A., van der Kruk, J., Vanderborght, J., Caers, J., ... & Englert, A. (2017). High resolution aquifer characterization using crosshole GPR full-waveform tomography: Comparison with direct-push and tracer test data. *Water Resources Research*, 53(1), 49–72.
- Hermans, T., Lesparre, N., De Schepper, G., & Robert, T. (2019). Bayesian evidential learning: a field validation using push-pull tests. *Hydrogeology Journal*, 27(5), 1661–1672.

- Hermans, T., Wildemeersch, S., Jamin, P., Orban, P., Brouyère, S., Dassargues, A., & Nguyen, F. (2015). Quantitative temperature monitoring of a heat tracing experiment using cross-borehole ERT. *Geothermics*, 53, 14–26.
- Hoffmann, R., Goderniaux, P., Jamin, P., Chatton, E., Bernardie, J., Labasque, T., et al. (2020). Continuous Dissolved Gas Tracing of Fracture-Matrix Exchanges. *Geophysical Research Letters*, 47(17), e2020GL0889441.
- Irvine, D. J., Simmons, C. T., Werner, A. D., & Graf, T. (2015). Heat and Solute Tracers: How Do They Compare in Heterogeneous Aquifers? *Groundwater*, 53(S1), 10–20.
- Kelter, M., Huisman, J. A., Zimmermann, E., & Vereecken, H. (2018). Field evaluation of broadband spectral electrical imaging for soil and aquifer characterization. *Journal of Applied Geophysics*, 159, 484–496.
- Kemna, A., Vanderborght, J., Kulesa, B., & Vereecken, H. (2002). Imaging and characterisation of subsurface solute transport using electrical resistivity tomography (ERT) and equivalent transport models. *Journal of Hydrology*, 267(3–4), 125–146.
- Klepikova, M. V., Le Borgne, T., Bour, O., Dentz, M., Hochreutener, R., & Lavenant, N. (2016). Heat as a tracer for understanding transport processes in fractured media: Theory and field assessment from multiscale thermal push-pull tracer tests. *Water Resources Research*, 52(7), 5442–5457.
- Klotzsche, A., Vereecken, H., & van der Kruk, J. (2019). Review of crosshole ground-penetrating radar full-waveform inversion of experimental data: Recent developments, challenges, and pitfalls. *Geophysics*, 84(6), H13–H28.
- Kurylyk, B. L., & Irvine, D. J. (2019). Heat: An Overlooked Tool in the Practicing Hydrogeologist's Toolbox. *Groundwater*, 57(4), 517–524.
- Li, W., Englert, A., Cirpka, O. A., & Vereecken, H. (2008). Three-dimensional geostatistical inversion of flowmeter and pumping test data. *Groundwater*, 46(2), 193–201.
- Looms, M. C., Jensen, K. H., Binley, A., & Nielsen, L. (2008). Monitoring unsaturated flow and transport using cross-borehole geophysical methods. *Vadose Zone Journal*, 7(1), 227–237.
- Ma, R., & Zheng, C. (2010). Effects of density and viscosity in modeling heat as a groundwater tracer. *Ground Water*, 48(3), 380–389.
- Maliva, R. G. (2016). *Aquifer Characterization Techniques*. Cham: Springer International Publishing.
- Müller, K., Vanderborght, J., Englert, A., Kemna, A., Huisman, J. A., Rings, J., & Vereecken, H. (2010). Imaging and characterization of solute transport during two tracer tests in a shallow aquifer using electrical resistivity tomography and multilevel groundwater samplers. *Water Resources Research*, 46(3).
- Oberhörmann, M., Klotzsche, A., Vereecken, H., & van der Krak, J. (2013). Optimization of acquisition setup for cross-hole: GPR full-waveform inversion using checkerboard analysis. *Near Surface Geophysics*, 11(2), 197–209.
- Ptak, T., Piepenbrink, M., & Martac, E. (2004). Tracer tests for the investigation of heterogeneous porous media and stochastic modelling of flow and transport—a review of some recent developments. *Journal of Hydrology*, 294(1–3), 122–163.
- Read, T., Bour, O., Bense, V., Le Borgne, T., Goderniaux, P., Klepikova, M. V., et al. (2013). Characterizing groundwater flow and heat transport in fractured rock using fiber-optic distributed temperature sensing. *Geophysical Research Letters*, 40(10), 2055–2059.
- Sarris, T. S., Close, M., & Abraham, P. (2018). Using solute and heat tracers for aquifer characterization in a strongly heterogeneous alluvial aquifer. *Journal of Hydrology*, 558, 55–71.

- Shakas, A., Linde, N., Baron, L., Bochet, O., Bour, O., & Le Borgne, T. (2016). Hydrogeophysical characterization of transport processes in fractured rock by combining push-pull and single-hole ground penetrating radar experiments. *Water Resources Research*, 52(2), 938-953.
- Skagius, K., & Neretnieks, I. (1986). Porosities and Diffusivities of Some Nonsorbing Species in Crystalline Rocks. *Water Resources Research*, 22(3), 389–398.
- Tillmann, A., Englert, A., Nyari, Z., Fejes, I., Vanderborght, J., & Vereecken, H. (2008). Characterization of subsoil heterogeneity, estimation of grain size distribution and hydraulic conductivity at the Krauthausen test site using cone penetration test. *Journal of Contaminant Hydrology*, 95(1-2), 57-75.
- Vanderborght, J., & Vereecken, H. (2001). Analyses of locally measured bromide breakthrough curves from a natural gradient tracer experiment at Krauthausen. *Journal of Contaminant Hydrology*, 48(1-2), 23-43.
- Vereecken, H., Döring, U., Hardelauf, H., Jaekel, U., Hashagen, U., Neuendorf, O., et al. (2000). Analysis of solute transport in a heterogeneous aquifer: the Krauthausen field experiment. *Journal of Contaminant Hydrology*, 45(3–4), 329–358.
- Wagner, V., Li, T., Bayer, P., Leven, C., Dietrich, P., & Blum, P. (2014). Thermal tracer testing in a sedimentary aquifer: field experiment (Lauswiesen, Germany) and numerical simulation. *Hydrogeology Journal*, 22(1), 175–187.
- Wildemeersch, S., Jamin, P., Orban, P., Hermans, T., Klepikova, M., Nguyen, F., et al. (2014). Coupling heat and chemical tracer experiments for estimating heat transfer parameters in shallow alluvial aquifers. *Journal of Contaminant Hydrology*, 169, 90–99.

End of deliverable WP4 D4.2 D10



Enigma ITN

WP4 D4.2 / D10